

# BREEN: Bridge Data-Efficient Encoder-Free Multimodal Learning with Learnable Queries

♦ Tianle Li, ♥ Yongming Rao\*, ♥ Winston Hu, ♦ Yu Cheng\*  
 ♦ The Chinese University of Hong Kong, ♥ Tencent Hunyuan Research

tianleli@link.cuhk.edu.hk

<https://github.com/lt13A87/BREEN>

## Abstract

Encoder-free multimodal large language models (MLLMs) eliminate the need for a well-trained vision encoder by directly processing image tokens before the language model. While this approach reduces computational overhead and model complexity, it often requires large amounts of training data to effectively capture the visual knowledge typically encoded by vision models like CLIP. The absence of a vision encoder implies that the model is likely to rely on substantial data to learn the necessary visual-semantic alignments. In this work, we present BREEN, a data-efficient encoder-free multimodal architecture that mitigates this issue. BREEN leverages a learnable query and image experts to achieve comparable performance with significantly less training data. The learnable query, positioned between image and text tokens, is supervised by the output of a pretrained CLIP model to distill visual knowledge, bridging the gap between visual and textual modalities. Additionally, the image expert processes image tokens and learnable queries independently, improving efficiency and reducing interference with the LLM’s textual capabilities. BREEN achieves comparable performance to prior encoder-free state-of-the-art models like Mono-InternVL, using only 13 million text-image pairs in training—about one percent of the data required by existing methods. Our work highlights a promising direction for data-efficient encoder-free multimodal learning, offering an alternative to traditional encoder-based approaches.

## 1. Introduction

Multimodal large language models (MLLMs) have shown impressive capabilities in understanding and generating text conditioned on visual inputs [1, 2, 10, 29, 38, 42]. Traditional approaches rely on vision encoders, such as CLIP [33], to extract encoded visual representations, which are then fused

\*Corresponding authors.

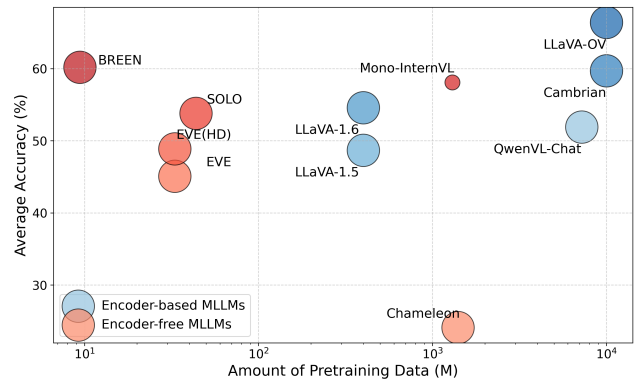


Figure 1. Comparison of encoder-based and encoder-free multimodal large language models (MLLMs) in terms of pretraining data volume, average accuracy on evaluation benchmarks, and model size. The x-axis represents the amount of pretraining data (in millions) on a logarithmic scale, while the y-axis shows the average accuracy (%). The size of each circle corresponds to the model’s LLM backbone size.

with textual inputs within a language model as shown in section (a) in Figure 2 [24–26]. While this paradigm achieves strong performance across various vision-language tasks, it introduces significant computational overhead and complexity, particularly during inference. The reliance on an explicit vision encoder not only necessitates additional processing steps but also constrains the visual capabilities due to information loss, hindering real-time applications [8]. Consequently, researchers have explored alternative architectures that aim to reduce computational burden and loss of visual information, while maintaining competitive performance [5, 8, 12, 31].

To address these limitations, encoder-free architectures have recently gained traction as a more integral alternative. Notable pioneering works such as EVE [12] and Fuyu [5] eliminate the explicit vision encoder and instead directly feed image patches into the LLM after MLP layers or shallow

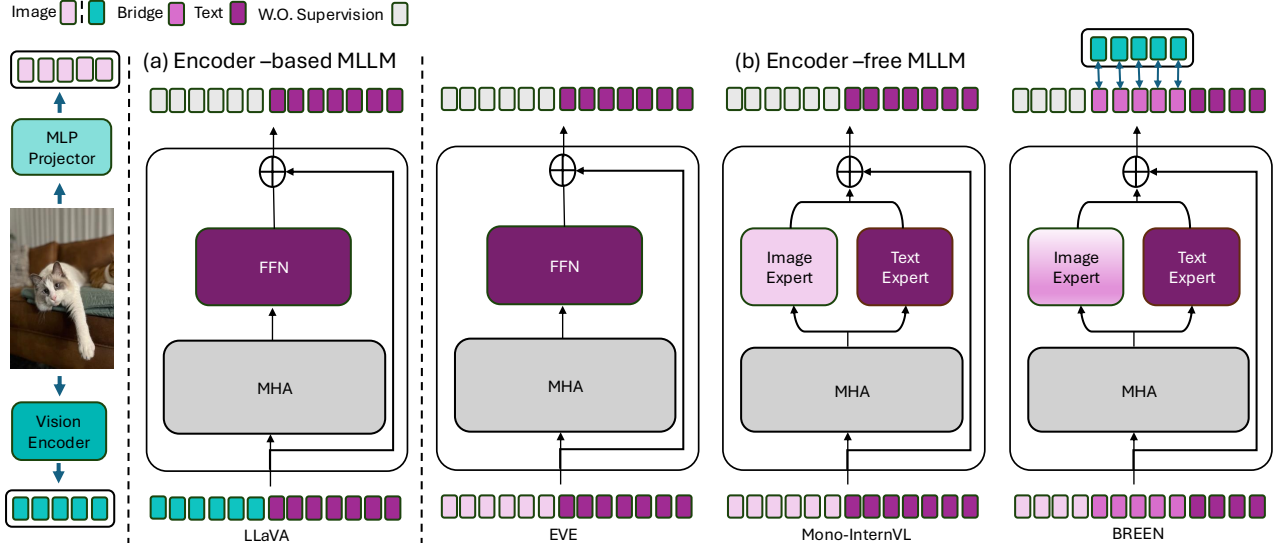


Figure 2. Comparison among different architectures. For Encoder-based MLLMs, we choose the series of LLaVA [22, 24, 25] as the representative. It feeds the images to the well-trained vision encoder, and project the outputs into the input space of the base LLM. For Encoder-free MLLMs, we choose previous works as EVE [12] and Mono-InternVL [31] to compare. Instead of encoding the images with a vision encoder, these models use simpler and shallow patch embedding layers to encode the image patch directly.

patch embedding layers. This design simplifies the processing pipeline and enhances inference efficiency by treating image and text inputs within a unified framework. However, despite these advantages, encoder-free models often underperform compared to their encoder-based counterparts. This performance gap is largely attributed to the absence of aligned visual features from well-trained encoders, such as CLIP or SigLIP [33, 48], which inherently capture high-level semantics from image inputs through extensive pretraining. A concurrent work, Mono-InternVL [31], attempts to mitigate this issue by incorporating image experts that process vision tokens separately from text tokens. Combined with large-scale pretraining on billions of text-image pairs, this approach improves alignment and enhances multimodal reasoning from scratch without relying on the extraction of the image features from vision encoder. However, such extensive pretraining is resource-intensive, taking 256 A100 GPUs 16 days to complete the pretraining.

In this work, we introduce **BREEN**, a **data-efficient encoder-free multimodal architecture** that effectively distills knowledge from vision encoders while maintaining strong performance with significantly **fewer training resources**. Our key innovation is a **learnable query**, positioned between image and text tokens, which serves as a bridge for transferring semantic knowledge from a pretrained CLIP model during the pre-aligning and pretraining stages. Unlike prior encoder-free models that require massive datasets to learn alignment from scratch, BREEN efficiently **leverages only 13 million text-image pairs in total for pre-training**

**and SFT**, substantially reducing data requirements while achieving superior performance. To further enhance vision interactions, we introduce an **image expert** that processes both image tokens and learnable queries independently, minimizing interference with the LLM’s core textual reasoning capabilities. As shown in Figure 1, these designs enable **BREEN to achieve state-of-the-art performance among encoder-free models while being significantly more data-efficient**, avoiding the need for extensive multimodal pretraining.

Additionally, we observe that the granularity of the learnable query is crucial for different multimodal tasks. Fine-grained CLIP features are beneficial for spatially aware tasks such as OCR and geometric reasoning [28, 32], whereas coarse-grained representations are more suitable for high-level perceptual tasks like color recognition [16]. To balance this trade-off, we concatenate both fine-grained and coarse-grained learnable queries into a single sequence, allowing the learnable queries to align with representations of different granularity simultaneously. This mechanism ensures strong performance across a diverse range of multimodal tasks. To further validate the effectiveness of learnable queries in multimodal reasoning and understanding, we analyze the model’s attention patterns on image tokens and learnable query tokens. The visualization demonstrates that learnable queries play a crucial role in refining attention to relevant image regions, which may provide a more intuitive explanation on the reason why the inclusion of the learnable queries can enhance the performance.

With a training dataset comprising approximately **13 million** text-image pairs across the pre-aligning, pretraining, and SFT stages, BREEN surpasses prior encoder-free models such as EVE(HD) and Mono-InternVL, achieving a **2% performance improvement** on average across multiple multimodal benchmarks, including MMMU, MME, MMVet, GQA, AI2D, MMB, MMStar, etc. [7, 16, 19, 20, 27, 46, 47].

Our contributions can be summarized as follows:

- We propose a novel encoder-free architecture BREEN that leverages a learnable query to transfer visual knowledge from a pretrained CLIP model, bridging the performance gap between encoder-based and encoder-free models while maintaining inference efficiency.
- We discover that the combination of fine-grained and coarse-grained learnable queries can enhance multimodal understanding across diverse tasks. Attention visualizations further demonstrate that learnable queries effectively refine vision-language alignment, improving reasoning capabilities.
- With only 13 million text-image pairs, BREEN achieves superior results compared to prior encoder-free models, demonstrating the effectiveness of our approach in balancing efficiency and performance.

Our work establishes a promising direction toward **data-efficient** multimodal learning, providing a potential alternative to traditional encoder-based MLLMs.

## 2. Related Work

### 2.1. Vision-Encoder-Based Multimodal Models

Recent advances in large language models (LLMs) [11, 14, 45] have fueled the integration of vision and language modalities, resulting in multimodal large language models. Notable commercial models such as GPT-4V [2], Claude 3.5 [1], and Gemini [38], as well as open-source models like LLaVA [24–26], DeepSeek-VL [29, 34], QwenVL [4, 42], and InternVL [9, 10], typically rely on vision encoder like CLIP [33] for visual feature extraction. These models integrate visual and textual information by mapping vision features into the input space of LLMs, achieving strong performance across various vision-language tasks. However, these encoder-based models face significant challenges, particularly related to computational inefficiency and the limitations of pre-trained vision encoders. The reliance on pre-trained visual encoders often results in the loss of task-specific visual information, limiting model flexibility and hindering adaptation to new domains [8].

### 2.2. Encoder-Free Multimodal Models

The challenges associated with modular MLLMs have driven research toward encoder-free architectures, which aim to eliminate the need for explicit vision encoders while maintaining strong performance in multimodal tasks. Encoder-

free models focus on obtaining continuous visual tokens through a lightweight structure before feeding them into the LLM. For instance, Fuyu-8B [5] processes images directly via a simple linear projection, handling high-resolution images effectively without requiring a vision encoder. Similarly, EVE-7B [12] designs a shallow patch embedding layers to deal with image input and enhance image feature learning through visual alignment in hidden layers. SOLO [8] presents a simple linear projection to transfer images into continuous embeddings similar to Fuyu. Mono-InternVL [31] takes a different approach by embedding new visual parameters into a pretrained LLM, integrating visual experts via a multimodal mixture-of-experts [35] structure. These models represent a possible alternative to traditional vision-encoder-based MLLMs, significantly reducing the computational overhead for the encoding of image features while enabling end-to-end multimodal processing. Another series works like Chameleon [37], Show-o [44], and EMU3 [43], on the other hand, leverage pre-trained discrete visual tokenizer [15, 41] to encode images into tokens and feed into LLMs after concatenation with text tokens.

### 2.3. Data Efficiency in Multimodal Learning

Data efficiency is essential in the development of multimodal models, especially as training large-scale models becomes resource-intensive. Approaches like Bunny [18] and ALLaVA [6] emphasize the use of curated datasets or synthetic data to reduce the need for large amounts of labeled data, achieving competitive performance with fewer examples. In contrast, Mono-InternVL [31] achieves strong performance by leveraging large datasets (e.g., 1.3B examples) to learn image-text alignment in the absence of a pretrained image encoder. Our work addresses this by utilizing a pretrained image encoder like CLIP and a learnable query to efficiently learn image-text representations with less data. While larger datasets could further improve performance, our method offers a more data-efficient alternative while maintaining strong performance across vision-language tasks.

## 3. Method

In this section, we describe the architecture design of BREEN and its training methodology as shown in Figure 3. BREEN introduces a novel encoder-free multimodal framework that integrates learnable queries in the auto-regressive learning objective and involves an image expert to process both image tokens and learnable query tokens, so that enhancing vision-language alignment. Similarly to previous work [12], our training pipeline consists of three stages: pre-aligning, pretraining, and supervised fine-tuning (SFT), each contributing to aligning and enhancing the multimodal reasoning capability of the model.

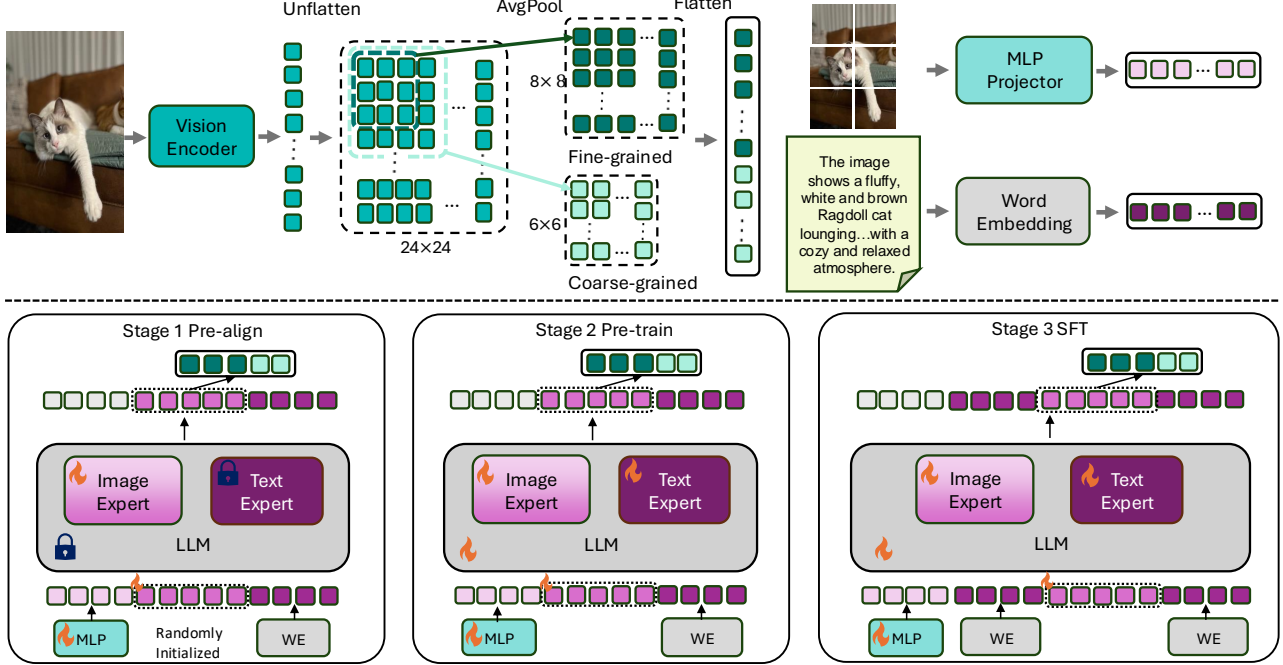


Figure 3. Overview of the proposed BREEN framework.

### 3.1. BREEN Architecture

BREEN follows an encoder-free multimodal paradigm, where images are tokenized into patches and directly fed into the LLM. To bridge the modality gap, we introduce a set of learnable query tokens ( $\mathbf{Q}$ ) that act as intermediaries between image and text tokens. These queries are supervised by the CLIP-derived visual representations ( $\mathbf{V}_{\text{CLIP}}$ ), ensuring effective transfer of visual semantics to the LLM.

**Image tokenization and learnable queries** As shown in Figure 3, images are first divided into patches of size  $P \times P$ , which are then projected into embeddings through an MLP layer before being input to the model. Learnable query tokens are inserted between image and text embeddings, facilitating the extraction of meaningful visual knowledge from CLIP. The length of the learnable queries depends on the granularity of the supervision from CLIP  $\mathbf{V}_{\text{CLIP}}$ .

To derive structured visual information as supervision for the learnable queries, the input image is resized and padded to CLIP’s required resolution ( $336 \times 336$ ), producing a feature representation of size  $24 \times 24$  after being fed to CLIP encoder with a patch size of 14. This feature grid is then unflattened into a two-dimensional structure.

For finer-grained mappings, a patch size and stride of 3 are applied, resulting in a flattened sequence  $\mathbf{V}_{\text{CLIP}}^{\text{fine}}$  of 64 tokens ( $8 \times 8$ ) as shown in the upper left part in Figure 3. Coarse-grained alignment, using a patch size and stride of 4,

produces a sequence  $\mathbf{V}_{\text{CLIP}}^{\text{coarse}}$  of 36 tokens ( $6 \times 6$ ). To ensure adaptability across different multimodal tasks, BREEN concatenates randomly initialized fine-grained learnable query  $\mathbf{Q}^{\text{fine}}$  and coarse-grained learnable query  $\mathbf{Q}^{\text{coarse}}$  into a single sequence  $\mathbf{Q}$  of length 100 ( $64 + 36$ ). These query tokens are positioned after image patches but before text tokens during pretraining, allowing the model to dynamically utilize the appropriate level of visual abstraction through its attention mechanism.

**Alignment loss and knowledge transfer** To ensure effective knowledge transfer, the output representations of learnable queries ( $\mathbf{Q}_{\text{out}}$ ) after LLM processing are aligned with their corresponding CLIP-derived embeddings ( $\mathbf{V}_{\text{CLIP}}$ ) using cosine similarity loss:

$$\mathcal{L}_{\text{align}}^* = 1 - \frac{\mathbf{Q}_{\text{out}}^* \cdot \mathbf{V}_{\text{CLIP}}^*}{\|\mathbf{Q}_{\text{out}}^*\| \|\mathbf{V}_{\text{CLIP}}^*\|} \quad (1)$$

where  $\mathbf{Q}_{\text{out}}^*$  denotes the learnable query representations after passing through the LLM and a linear projection, and  $\mathbf{V}_{\text{CLIP}}^*$  represents the corresponding CLIP image embeddings. The symbol  $*$  represents the granularity level (fine or coarse). The overall alignment loss is defined as:

$$\mathcal{L}_{\text{align}} = \mathcal{L}_{\text{align}}^{\text{coarse}} + \mathcal{L}_{\text{align}}^{\text{fine}} \quad (2)$$

The final training objective combines this loss with the standard autoregressive language modeling loss ( $\mathcal{L}_{\text{LM}}$ ) for

text tokens, where  $\alpha$  and  $\beta$  is the weights for alignment loss and LM loss:

$$\mathcal{L} = \alpha\mathcal{L}_{\text{align}} + \beta\mathcal{L}_{\text{LM}} \quad (3)$$

**Image expert for modality-specific processing** To ensure that image patches and learnable queries are processed effectively without interfering with the LLM’s core text processing, an image expert is introduced into the feed-forward network (FFN) of each transformer layer. This specialized expert enables more refined vision-language interactions while better preserving the LLM’s original text-based reasoning capabilities.

### 3.2. Training Strategy

BREEN undergoes three sequential training stages to optimize its multimodal alignment and understanding.

**1. Pre-Aligning Stage** In this stage, we initialize the model using a pretrained large language model (LLM) backbone. To stabilize early-stage training, only the learnable query tokens, image linear projector, and image expert weights are updated, while all other parameters remain frozen. The goal is to align the learnable queries with CLIP representation, and simultaneously, force the image linear projector and image expert to align the image features to the caption space. This stage ensures that the new parameters provide a strong starting point for effective image understanding. This alignment helps establish a solid foundation for the subsequent multimodal training, leveraging the well-initialized LLM parameters before fine-tuning the entire model. We collect 9 million of image-text pairs randomly selected from BLIP3-KALE [3], and randomly draw 4 millions out of 9 millions for training in the pre-aligning stage.

**2. Pretraining Stage** Once the pre-alignment is achieved, all model parameters are unfrozen, and BREEN is trained on larger-scale image-text caption pairs. The model jointly optimizes the alignment loss ( $\mathcal{L}_{\text{align}}$ ) and the language modeling loss ( $\mathcal{L}_{\text{LM}}$ ) to reinforce the connection between visual semantics and textual understanding. In the pretraining stage, we make full use of the 9 millions of image-text pairs as mentioned above from BLIP3-KALE to train the model.

**3. Supervised Fine-Tuning (SFT) Stage** In the final stage, BREEN is fine-tuned using multimodal instruction datasets with all the parameters unfrozen. To make the learnable query look ahead at the task context according to the casual mask mechanism, we pre-append the instruction text before the learnable queries and after image patches as shown in the last stage in Figure 3, enabling the model to infer the appropriate granularity based on task context as the text instruction

and image tokens. In this stage, we gather 4 million of image-text instruction following datasets from open-source public datasets, including Cambrian-1 [39], LLaVAOneVision [23], and Cauldron [21] to fine-tune the model.

Through these three stages, BREEN effectively bridges the vision-language gap, achieving strong multimodal reasoning capabilities while preserving the efficiency of encoder-free architectures.

## 4. Experiment

### 4.1. Implementation Details

Our BREEN model is based on Qwen2.5-7B-Instruct, where the weights of image expert are initialized from the feed-forward layer in the LLM. The target of learnable queries are extracted by feeding corresponding images to clip-vit-large-patch14. The learning rates for pre-aligning, pre-training and SFT are  $4 \times 10^{-4}$ ,  $4 \times 10^{-5}$ , and  $4 \times 10^{-5}$  respectively. The batch size for these three stages are 512, 512, and 256 correspondingly. In pre-aligning and pre-training stage, we set  $\alpha = 1$  and  $\beta = 1$  in Equation 3 for aligning loss and LLM loss. In SFT stage, we set  $\alpha = 0.5$  and  $\beta = 1$  to focus more on text generation. The whole training process takes four nodes of 8×A800 GPUs 16 days to finish.

### 4.2. Evaluation Benchmarks

In this work, we evaluate our model using a diverse set of multimodal benchmarks to assess its performance across various image-text understanding tasks. The evaluation benchmarks include MMMU[47], MMB<sup>en</sup> (MMBench-EN)[27], MMV (MMVet)[46], MME[16], SQA<sup>1</sup> (ScienceQA-Img)[30], TVQA[36], HallB (HallusionBench)[17], AI2D[20], and MMS (MMStar) [7]. These datasets provide a comprehensive suite of challenges for multimodal models, testing their ability to handle a wide range of reasoning tasks involving both visual and textual inputs. We harness a standard and efficient evaluation toolkit lmms-eval<sup>1</sup> to conduct the evaluation for BREEN. For the other competitors, some of the results are directly obtained from the Open VLM Leaderboard<sup>2</sup>, and the other of them are evaluated with VLMEvalKit [13].

### 4.3. Main Result Analysis

We compare the performance of BREEN against previous multimodal large language models across various multimodal benchmarks. Table 1 presents the results in terms of accuracy for each task and the overall average scores after normalizing the scale of the tasks. Generally, BREEN achieves an average score of 60.2, outperforming all other encoder-free MLLMs and demonstrating competitive results

<sup>1</sup><https://github.com/EvolvingLMs-Lab/lmms-eval>.

<sup>2</sup><https://huggingface.co/spaces/opencompass/opencompass-llm-leaderboard>

even against encoder-based models. Although encoder-based models generally achieve higher scores due to explicit vision encoders, BREEN narrows this gap, performing comparably to Cambrian (59.7) while remaining behind LLaVA-OV (66.4), which benefits from significantly larger pretraining data (10B+ image-text pairs).

Among encoder-free MLLMs, BREEN consistently achieves the highest accuracy on half of the selected benchmarks and is placed second on the other half. Notably, BREEN improves significantly over Mono-InternVL, with a 9% increase on MMMU (33.7  $\rightarrow$  42.7), a 5.9% gain on MMBench-EN (65.5  $\rightarrow$  71.4), a 7.8% increase on AI2D (68.6  $\rightarrow$  76.4), and a 5.2% improvement on MMStar (46.0  $\rightarrow$  51.2). When placed second, BREEN remains only slightly behind the best encoder-free model most of the time, with a 1.2% difference on MMVet (40.1 vs. 38.9), 0.2% on ScienceQA-Img (93.6 vs. 93.4), and 0.8% on GQA (62.6 vs. 61.8). Although Mono-InternVL has a smaller model size (1.8B vs. 7B), it has undergone pretraining on more than 100 times the data compared to BREEN, demonstrating the latter’s remarkable data efficiency while maintaining competitive performance.

According to the comparison, we can discover that a key advantage of BREEN is its data efficiency. While encoder-based models such as Cambrian and LLaVA-OV rely on 10B+ pretraining samples, BREEN achieves competitive results using only 9M pretraining samples, a fraction of the data required by the encoder-based models.

We further visualize performance improvements if the amount of data increases from 4M to 9M in the pre-training stage in Figure 4. We can observe that even with merely 4M pretraining data, BREEN can outperform Mono-InternVL on MMMU, MMB, GQA, AI2D and MMStar. In addition, it also shows a great potential that the performance of BREEN can be further boosted if we continue to expand the amount of pretraining data. In a nutshell, despite its much smaller training corpus, BREEN demonstrates strong generalization, particularly excelling in high-level reasoning and multimodal understanding tasks, validating the effectiveness of its learnable query mechanism in distilling multimodal knowledge without requiring an explicit vision encoder.

#### 4.4. Ablation Studies

To evaluate the contribution of various components in the BREEN architecture, we conduct an ablation study as shown in Table 2. The study focuses on the impact of different architectural decisions, such as the inclusion of the image expert, the use of learnable queries supervised by CLIP outputs at different granularities, and the concatenation of multi-grained learnable queries to balance the performance across various types of tasks. Due to the limited computational resources, we conduct all the ablation studies with the base

model Qwen2.5-1.5B-Instruct<sup>3</sup>, and leverage a subset of training data, specifically, 4M/4M/1M for the three stages respectively to train the model. The performance metrics are reported across several multimodal benchmarks, including SQA<sup>I</sup>, TQA, GQA, and MME.

**Impact of Image Expert** The first and the second row in Table 2 demonstrates that the inclusion of the image expert significantly boosts the model’s performance across all datasets. The image expert, which processes image tokens independently, helps the model better handle the visual modality and aligns it more effectively with textual tokens, leading to notable improvements. For instance, the performance on the SQA<sup>I</sup> task jumps from 55.3 to 62.4 with the image expert, while performance on TQA increases from 35.8 to 40.0.

#### Effect of Learnable Queries with Different Granularity

When we introduce **learnable queries (LQ)** based on different granularity of CLIP outputs, we observe a further performance boost. Specifically, in the third, fourth, and fifth rows of Table 2, we use learnable queries to align with the representations extracted from CLIP output with different stride sizes (LQ(Str2), LQ(Str3) and LQ(Str4)). The performance of the model on SQA<sup>I</sup> increases from 62.4 to 63.3 with LQ(Str3), and is maintained similar when adding LQ(Str2) or LQ(Str4). For all the other three datasets, we can observe a consistent improvement after integrating learnable queries with different granularity. It is worth noting that not a single granularity of learnable queries can achieve the best performance among all the datasets.

Next, we concatenate the learnable queries from two of the granularity (LQ(Str3) and LQ(Str4)) into a single sequence, as shown in the sixth row of Table 2. The performance on each evaluation dataset either maintains as the higher one or surpasses the individual results from stride 3 and stride 4. For example, the performance on SQA<sup>I</sup> increases to 63.7 when concatenating the queries, and the accuracy on MME improves to 1333.4. This demonstrates that combining different levels of granularity of visual knowledge with learnable queries allows the model to benefit from the complementary strengths of fine-grained and coarse-grained representations, leading to a more robust multimodal model. Other than directly concatenation, we also explore other ways of multi-grain alignment and ablate the order of granularity, which is demonstrated in Appendix A.1. While BREEN presents a significant step toward data-efficient encoder-free MLLMs, several limitations remain. We discuss the potential limitations and future plans in Appendix A.4.

<sup>3</sup><https://huggingface.co/Qwen/Qwen2.5-1.5B-Instruct>

Method	#Param	#Data	MMMU	MMB <sup>en</sup>	MMV	MME	GQA	SQA <sup>I</sup>	TQA	HallB	AI2D	MMS	Avg
<i>Encoder-based MLLMs:</i>													
LLaVA-1.5	7B	0.4B+ / 665K	35.3	64.3	30.5	1859	62.0	66.8	46.1	27.6	54.8	33.1	48.7
QwenVL-Chat	7B	7.2B / 50M	35.9	60.6	–	1848	57.5	68.2	61.5	<b>36.8</b>	45.9	34.5	51.9
LLaVA-1.6	7B	0.4B+ / 760K	35.1	67.4	<u>43.9</u>	1842	<u>64.2</u>	70.2	64.9	29.1	66.6	38.4	54.6
Cambrian	7B	10B+ / 7M	42.7	75.9	48.0	–	<b>64.6</b>	80.4	<b>71.7</b>	30.6	73.0	50.7	<u>59.7</u>
LLaVA-OV	7B	10B+ / 3.2M	<b>47.3</b>	<b>81.7</b>	<b>58.8</b>	<b>1998</b>	–	<b>96.6</b>	–	<u>31.6</u>	<b>81.6</b>	<b>61.9</b>	<b>66.4</b>
<i>Encoder-free MLLMs:</i>													
Chameleon	7B	1.4B+ / 1.8M	25.4	31.1	8.3	170	–	47.2	4.8	17.1	46.0	31.1	24.1
Fuyu	8B	– / –	27.9	10.7	21.4	–	–	–	–	–	64.5	34.4	31.8
EVE	7B	33M / 665K	32.3	49.5	25.6	1483	60.8	63.0	51.9	21.1	48.5	–	45.1
EVE(HD)	7B	33M / 1.8M	32.6	52.3	25.7	1628	<b>62.6</b>	64.9	56.8	26.4	61.0	–	48.9
SOLO	8B	43.7M / 2M	–	–	–	1260	–	73.3	–	–	61.4	35.5	53.8
Emu3	8B	– / –	31.6	58.5	37.2	1611	60.3	89.2	64.7	31.7	<u>70.0</u>	<u>46.6</u>	54.7
Mono-InternVL	1.8B	1.3B / 7M	<u>33.7</u>	<u>65.5</u>	<b>40.1</b>	<b>1875</b>	59.5	<b>93.6</b>	<b>72.6</b>	<u>34.8</u>	68.6	46.0	<u>58.1</u>
<b>BREEN</b>	7B	9M / 4M	<b>42.7</b>	<b>71.4</b>	<u>38.9</u>	<u>1770</u>	<u>61.8</u>	<u>93.4</u>	<u>65.7</u>	<b>37.0</b>	<b>76.4</b>	<b>51.2</b>	<b>60.2</b>

Table 1. Comparison with previous multi-modal large language models on various multi-modal benchmarks. #Param denotes the number of parameters of the base LLM models the MLLMs deploy; #Data represents the number of text-images pairs for pre-training / fine-tuning respectively; The best results is marked in bold, and the second one is marked with underline.

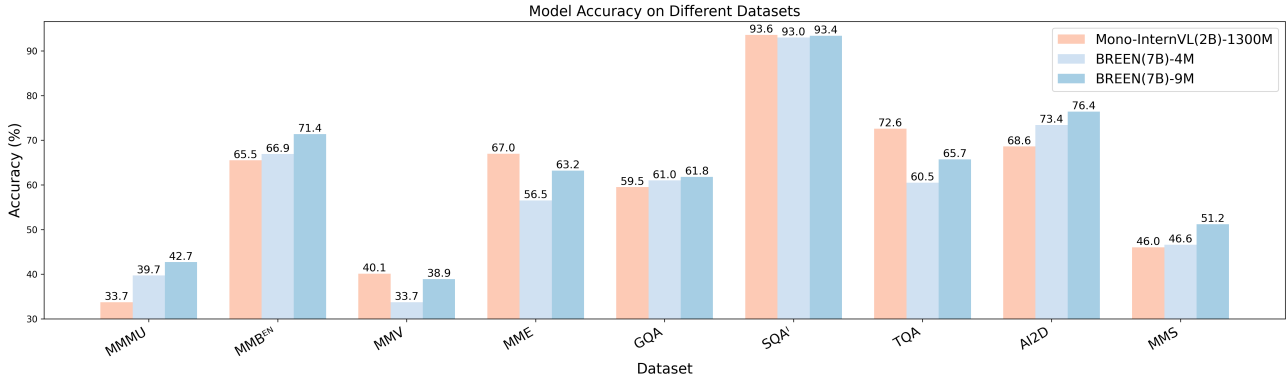


Figure 4. Comparison on the performance when the amount of pretraining data increases from 4M to 9M

**Effect of Granularity for Different Types of Tasks** To evaluate how different levels of query granularity affect performance across various tasks, we examine the results on the MMVet dataset [46], as shown in Table 3. The performance trends of the model vary significantly among tasks with different levels of granularity for the learnable queries.

For tasks requiring recognition capabilities, such as object identification, we observe that coarser granularity (with a larger stride) leads to better performance. On the other hand, for tasks that demand finer details, such as Optical Character Recognition (OCR) or spatial relationship understanding, finer granularity (with stride 2) achieves superior results. Moreover, the trend of performance changes with granularity is either monotonically increasing or decreasing across the three levels, providing further validation of the observed behavior. When combining granularity with stride values of 3 and 4, we notice a complementary enhancement in performance for tasks like OCR, knowledge retrieval, and spatial reasoning, leading to an overall improvement in per-

formance across the dataset. We also provide the results on different sub-tasks for MME dataset in the Appendix A.2, where similar conclusion can be drawn with MMVet.

#### 4.5. Visualization and Analysis

To further investigate the role of learnable queries in multi-modal understanding tasks, we visualize the attention scores for both image tokens and learnable query tokens, as shown in Figure 5. The two examples are taken from the MMVet evaluation set and are correctly answered by BREEN. Since BREEN’s base model consists of 28 layers, we select the 14th layer as the middle layer for analysis.

For the visualization of learnable query tokens, we compute the attention score for each query token at the selected layer. We then unflatten the attention score sequence and interpolate each value according to the stride size to map it back to the original input image fed into CLIP. In the first row of Figure 5, the attention scores from the output token to the image in the middle layer highlight the positions of indi-

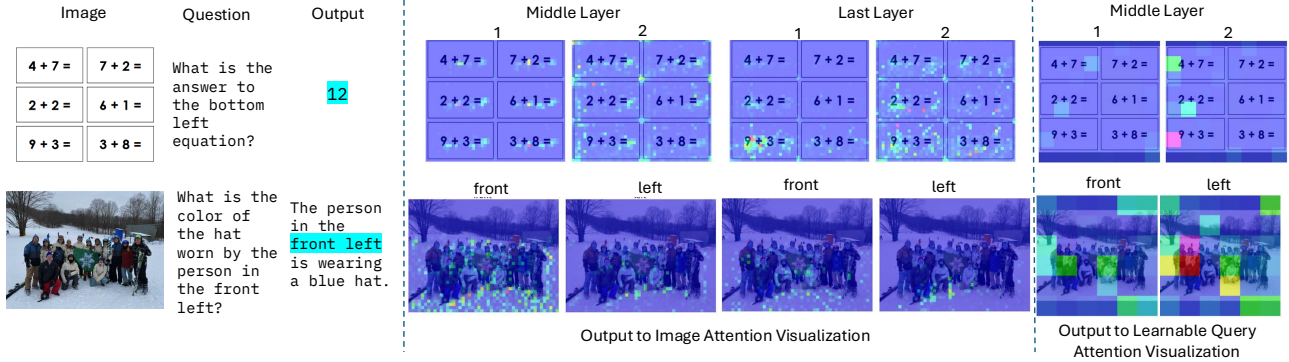


Figure 5. Visualization of attention scores from output tokens to image tokens and learnable query tokens.

Image Expert	LQ(Str2)	LQ(Str3)	LQ(Str4)	SQA <sup>1</sup>	TQA	GQA	MME
				55.3	35.8	48.9	1243.2
✓				62.4	40.0	50.8	1260.7
✓	✓			62.2	41.3	50.9	1284.3
✓		✓		63.3	41.1	51.7	1314.0
✓			✓	62.1	41.0	51.4	1284.9
✓		✓	✓	<b>63.7</b>	<b>41.4</b>	<b>51.7</b>	<b>1333.4</b>

Table 2. Ablation study of BREEN. **LQ(Str2)** means the target of learnable query tokens is extracted from average-pooling of image CLIP output with stride size 2, similar with **LQ(Str3)** and **LQ(Str4)**.

vidual equations. In the final layer, the attention weights shift focus more strongly toward the target equation in the bottom left. Similarly, in the visualization of output-to-learnable-query attention, the highest attention score corresponds to the beginning of the target equation (represented by the pink patch below output token “2”).

In the second row, where the model is tasked with identifying the color of a hat worn by a specific person, the output-to-image attention reveals that the “front” and “left” tokens do not precisely attend to the desired person in the front left; instead, they broadly distribute attention across those regions. In contrast, the attention to the learnable query accurately pinpoints the target person in the middle layer (indicated by the red patch below the output token “left”). The attention visualization for more layers of learnable query tokens can be found in Appendix A.3.2. These visualizations and observations provide insights into how the inclusion of learnable queries enhances multimodal understanding tasks.

## 5. Conclusion

In this work, we introduce BREEN, a data-efficient encoder-free multimodal architecture that leverages a learnable query to distill knowledge from a pretrained image encoder, mitigating the limitations of prior encoder-free models. Unlike traditional vision-encoder-based multimodal models, which suffer from computational inefficiencies and rigid visual representations, our approach eliminates the need for

a vision encoder while preserving strong visual-text alignment. Compared to existing encoder-free models like Mono-InternVL, which rely on large-scale datasets to learn image-text alignment from scratch, BREEN achieves competitive performance with significantly less data by efficiently transferring semantic information from well-trained image encoders. Experimental results show that BREEN surpasses previous encoder-free models while requiring fewer training resources, highlighting the effectiveness of leveraging pretrained vision models in an encoder-free setting. Future work includes scaling BREEN with larger datasets to explore its full potential, further refining the learnable query for improved representation learning, and extending the model to more complex multimodal reasoning tasks. Our findings pave the way for more data-efficient and scalable multimodal models, demonstrating that structured knowledge transfer from pretrained vision models can serve as a viable alternative to large-scale multimodal pretraining from scratch.

## References

- [1] The claude 3 model family: Opus, sonnet, haiku. 1, 3
- [2] OpenAI Josh Achiam, Steven Adler, Sandhini Agarwal, Lama Ahmad, Ilge Akkaya, Florencia Leoni Aleman, Diogo Almeida, Janko Altenschmidt, Sam Altman, Shyamal Anadkat, Red Avila, Igor Babuschkin, Suchir Balaji, Valerie Balcom, Paul Baltescu, Haim ing Bao, Mo Bavarian, Jeff Belgum, Irwan Bello, Jake Berdine, Gabriel Bernadett-Shapiro, Christopher Berner, Lenny Bogdonoff, Oleg Boiko, Made



Stride/Patch Size	Rec	OCR	Know	Gen	Spat	Math	Total
2 (12 × 12)	20.9	<u>7.8</u>	8.6	10.6	19.1	3.8	16.2
3 (8 × 8)	23	<u>7.8</u>	11.1	<b>13.1</b>	18.9	<b>7.7</b>	18.1
4 (6 × 6)	<b>24.3</b>	6.1	<u>11.8</u>	<b>13.1</b>	18.3	<b>7.7</b>	<u>18.6</u>
3 & 4 (8 × 8 + 6 × 6)	<u>23.1</u>	<b>8.6</b>	<b>12</b>	<u>12</u>	<b>19.3</b>	<b>7.7</b>	<b>18.7</b>

Table 3. Ablations of the influence of the stride sizes for learnable queries for different types of tasks in MMVet. The best score is highlighted by bold text and the second to best score is highlighted with the underline.

laine Boyd, Anna-Luisa Brakman, Greg Brockman, Tim Brooks, Miles Brundage, Kevin Button, Trevor Cai, Rosie Campbell, Andrew Cann, Brittany Carey, Chelsea Carlson, Rory Carmichael, Brooke Chan, Che Chang, Fotis Chantzis, Derek Chen, Sully Chen, Ruby Chen, Jason Chen, Mark Chen, Benjamin Chess, Chester Cho, Casey Chu, Hyung Won Chung, Dave Cummings, Jeremiah Currier, Yunxing Dai, Cory Decareaux, Thomas Degry, Noah Deutsch, Damien Deville, Arka Dhar, David Dohan, Steve Dowling, Sheila Dunning, Adrien Ecoffet, Atty Eleti, Tyna Eloundou, David Farhi, Liam Fedus, Niko Felix, Sim'on Posada Fishman, Juston Forte, Isabella Fulford, Leo Gao, Elie Georges, Christian Gibson, Vik Goel, Tarun Gogineni, Gabriel Goh, Raphael Gontijo-Lopes, Jonathan Gordon, Morgan Grafstein, Scott Gray, Ryan Greene, Joshua Gross, Shixiang Shane Gu, Yufei Guo, Chris Hallacy, Jesse Han, Jeff Harris, Yuchen He, Mike Heaton, Johannes Heidecke, Chris Hesse, Alan Hickey, Wade Hickey, Peter Hoeschele, Brandon Houghton, Kenny Hsu, Shengli Hu, Xin Hu, Joost Huizinga, Shantanu Jain, Shawn Jain, Joanne Jang, Angela Jiang, Roger Jiang, Haozhun Jin, Denny Jin, Shino Jomoto, Billie Jonn, Heewoo Jun, Tomer Kaftan, Lukasz Kaiser, Ali Kamali, Ingmar Kanitscheider, Nitish Shirish Keskar, Tabarak Khan, Logan Kilpatrick, Jong Wook Kim, Christina Kim, Yongjik Kim, Hendrik Kirchner, Jamie Ryan Kiros, Matthew Knight, Daniel Kokotajlo, Lukasz Kondraciuk, Andrew Kondrich, Aris Konstantinidis, Kyle Kosic, Gretchen Krueger, Vishal Kuo, Michael Lampe, Ikai Lan, Teddy Lee, Jan Leike, Jade Leung, Daniel Levy, Chak Ming Li, Rachel Lim, Molly Lin, Stephanie Lin, Ma teusz Litwin, Theresa Lopez, Ryan Lowe, Patricia Lue, Anna Makanju, Kim Malfacini, Sam Manning, Todor Markov, Yaniv Markovski, Bianca Martin, Katie Mayer, Andrew Mayne, Bob McGrew, Scott Mayer McKinney, Christine McLeavey, Paul McMillan, Jake McNeil, David Medina, Aalok Mehta, Jacob Menick, Luke Metz, Andrey Mishchenko, Pamela Mishkin, Vinnie Monaco, Evan Morikawa, Daniel P. Mossing, Tong Mu, Mira Murati, Oleg Murk, David M'ely, Ashvin Nair, Reiichiro Nakano, Rameesh Nayak, Arvind Neelakantan, Richard Ngo, Hyeonwoo Noh, Ouyang Long, Cullen O'Keefe, Jakub W. Pachocki, Alex Paino, Joe Palermo, Ashley Pantuliano, Giambattista Parascandolo, Joel Parish, Emy Parparita, Alexandre Passos, Mikhail Pavlov, Andrew Peng, Adam Perelman, Filipe de Avila Belbute Peres, Michael Petrov, Henrique Pondé de Oliveira Pinto, Michael Pokorny, Michelle Pokrass, Vitchyr H. Pong, Tolly Powell, Alethea Power, Boris Power, Elizabeth Proehl, Raul Puri, Alec Radford, Jack W. Rae, Aditya Ramesh,

Cameron Raymond, Francis Real, Kendra Rimbach, Carl Ross, Bob Rotsted, Henri Roussez, Nick Ryder, Mario D. Saltarelli, Ted Sanders, Shibani Santurkar, Girish Sastry, Heather Schmidt, David Schnurr, John Schulman, Daniel Selsam, Kyla Sheppard, Toki Sherbakov, Jessica Shieh, Sarah Shoker, Pranav Shyam, Szymon Sidor, Eric Sigler, Maddie Simens, Jordan Sitkin, Katarina Slama, Ian Sohl, Benjamin Sokolowsky, Yang Song, Natalie Staudacher, Felipe Petroski Such, Natalie Summers, Ilya Sutskever, Jie Tang, Nikolas A. Tezak, Madeleine Thompson, Phil Tillet, Amin Tootoonchian, Elizabeth Tseng, Preston Tuggle, Nick Turley, Jerry Tworek, Juan Felipe Cer'on Uribe, Andrea Vallone, Arun Vijayvergiya, Chelsea Voss, Carroll L. Wainwright, Justin Jay Wang, Alvin Wang, Ben Wang, Jonathan Ward, Jason Wei, CJ Weinmann, Akila Welihinda, Peter Welinder, Jiayi Weng, Lilian Weng, Matt Wiethoff, Dave Willner, Clemens Winter, Samuel Wolrich, Hannah Wong, Lauren Workman, Sherwin Wu, Jeff Wu, Michael Wu, Kai Xiao, Tao Xu, Sarah Yoo, Kevin Yu, Qiming Yuan, Wojciech Zaremba, Rowan Zellers, Chong Zhang, Marvin Zhang, Shengjia Zhao, Tianhao Zheng, Juntang Zhuang, William Zhuk, and Barret Zoph. Gpt-4 technical report. 2023. 1, 3

- [3] Anas Awadalla, Le Xue, Manli Shu, An Yan, Jun Wang, Senthil Purushwalkam, Sheng Shen, Hannah Lee, Oscar Lo, Jae Sung Park, Etash Guha, Silvio Savarese, Ludwig Schmidt, Yejin Choi, Caiming Xiong, and Ran Xu. Blip3-kale: Knowledge augmented large-scale dense captions, 2024. 5
- [4] Jinze Bai, Shuai Bai, Shusheng Yang, Shijie Wang, Sinan Tan, Peng Wang, Junyang Lin, Chang Zhou, and Jingren Zhou. Qwen-vl: A versatile vision-language model for understanding, localization, text reading, and beyond. 2023. 3
- [5] Rohan Bavishi, Erich Elsen, Curtis Hawthorne, Maxwell Nye, Augustus Odena, Arushi Somani, and Sağnak Taşlılar. Introducing our multimodal models, 2023. 1, 3
- [6] Guiming Hardy Chen, Shunian Chen, Ruifei Zhang, Junying Chen, Xiangbo Wu, Zhiyi Zhang, Zhihong Chen, Jianquan Li, Xiang Wan, and Benyou Wang. Allava: Harnessing gpt4v-synthesized data for lite vision-language models. 2024. 3
- [7] Lin Chen, Jinsong Li, Xiaowen Dong, Pan Zhang, Yuhang Zang, Zehui Chen, Haodong Duan, Jiaqi Wang, Yu Qiao, Dahua Lin, and Feng Zhao. Are we on the right way for evaluating large vision-language models? *ArXiv*, abs/2403.20330, 2024. 3, 5
- [8] Yangyi Chen, Xingyao Wang, Hao Peng, and Heng Ji. A single transformer for scalable vision-language modeling. *arXiv preprint arXiv:2407.06438*, 2024. 1, 3
- [9] Zhe Chen, Jiannan Wu, Wenhai Wang, Weijie Su, Guo Chen,

- Sen Xing, Muyan Zhong, Qinglong Zhang, Xizhou Zhu, Lewei Lu, Bin Li, Ping Luo, Tong Lu, Yu Qiao, and Jifeng Dai. Internvl: Scaling up vision foundation models and aligning for generic visual-linguistic tasks. *arXiv: 2312.14238*, 2023. 3
- [10] Zhe Chen, Weiyun Wang, Yue Cao, Yangzhou Liu, Zhangwei Gao, Erfei Cui, Jinguo Zhu, Shenglong Ye, Hao Tian, Zhaoyang Liu, Lixin Gu, Xuehui Wang, Qingyun Li, Yiming Ren, Zixuan Chen, Jiapeng Luo, Jiahao Wang, Tan Jiang, Bo Wang, Conghui He, Botian Shi, Xingcheng Zhang, Han Lv, Yi Wang, Wenqi Shao, Pei Chu, Zhongying Tu, Tong He, Zhiyong Wu, Hui Deng, Jiaye Ge, Kaiming Chen, Min Dou, Lewei Lu, Xizhou Zhu, Tong Lu, Dahu Lin, Yunfeng Qiao, Jifeng Dai, and Wenhai Wang. Expanding performance boundaries of open-source multimodal models with model, data, and test-time scaling. *ArXiv*, abs/2412.05271, 2024. 1, 3
- [11] DeepSeek-AI, Aixin Liu, Bei Feng, Bing Xue, Bing-Li Wang, Bochao Wu, Chengda Lu, Chenggang Zhao, Chengqi Deng, Chenyu Zhang, Chong Ruan, Damai Dai, Daya Guo, Dejian Yang, Deli Chen, Dong-Li Ji, Erhang Li, Fangyun Lin, Fucang Dai, Fuli Luo, Guangbo Hao, Guanting Chen, Guowei Li, H. Zhang, Han Bao, Hanwei Xu, Haocheng Wang, Haowei Zhang, Honghui Ding, Huajian Xin, Huazuo Gao, Hui Li, Hui Qu, J. L. Cai, Jian Liang, Jianzhong Guo, Jiaqi Ni, Jiashi Li, Jiawei Wang, Jin Chen, Jingchang Chen, Jingyang Yuan, Junjie Qiu, Junlong Li, Jun-Mei Song, Kai Dong, Kai Hu, Kaige Gao, Kang Guan, Kexin Huang, Kuai Yu, Lean Wang, Lecong Zhang, Lei Xu, Leyi Xia, Liang Zhao, Litong Wang, Liyue Zhang, Meng Li, Miaojun Wang, Mingchuan Zhang, Minghua Zhang, Minghui Tang, Mingming Li, Ning Tian, Panpan Huang, Peiyi Wang, Peng Zhang, Qiancheng Wang, Qihao Zhu, Qinyu Chen, Qiushi Du, R. J. Chen, R. L. Jin, Ruiqi Ge, Ruisong Zhang, Ruizhe Pan, Runji Wang, Runxin Xu, Ruoyu Zhang, Ruyi Chen, S. S. Li, Shanghao Lu, Shangyan Zhou, Shanhuang Chen, Shao-Ping Wu, Shengfeng Ye, Shiron Ma, Shiyu Wang, Shuang Zhou, Shuiping Yu, Shunfeng Zhou, Shuting Pan, T. Wang, Tao Yun, Tian Pei, Tianyu Sun, W. L. Xiao, Wangding Zeng, Wanbiao Zhao, Wei An, Wen Liu, Wenfeng Liang, Wenjun Gao, Wen-Xuan Yu, Wentao Zhang, X. Q. Li, Xiangyu Jin, Xianzu Wang, Xiaoling Bi, Xiaodong Liu, Xiaohan Wang, Xi-Cheng Shen, Xiaokang Chen, Xiaokang Zhang, Xiaosha Chen, Xiaotao Nie, Xiaowen Sun, Xiaoxiang Wang, Xin Cheng, Xin Liu, Xin Xie, Xingchao Liu, Xingkai Yu, Xinnan Song, Xinxia Shan, Xinyi Zhou, Xinyu Yang, Xinyuan Li, Xuecheng Su, Xuheng Lin, Y. K. Li, Y. Q. Wang, Y. X. Wei, Y. X. Zhu, Yang Zhang, Yanhong Xu, Yanping Huang, Yao Li, Yao Zhao, Yaofeng Sun, Yao Li, Yaohui Wang, Yi Yu, Yi Zheng, Yichao Zhang, Yifan Shi, Yi Xiong, Ying He, Ying Tang, Yishi Piao, Yisong Wang, Yixuan Tan, Yi-Bing Ma, Yiyuan Liu, Yongqiang Guo, Yu Wu, Yuan Ou, Yuchen Zhu, Yuduan Wang, Yue Gong, Yuheng Zou, Yujia He, Yukun Zha, Yunfan Xiong, Yunxiang Ma, Yuting Yan, Yu-Wei Luo, Yu mei You, Yuxuan Liu, Yuyang Zhou, Z. F. Wu, Zehui Ren, Zehui Ren, Zhangli Sha, Zhe Fu, Zhean Xu, Zhen Huang, Zhen Zhang, Zhenda Xie, Zhen guo Zhang, Zhewen Hao, Zhibin Gou, Zhicheng Ma, Zhigang Yan, Zhihong Shao, Zhipeng Xu, Zhiyu Wu, Zhongyu Zhang, Zhuoshu Li, Zihui Gu, Zijia Zhu, Zijun Liu, Zi-An Li, Ziwei Xie, Ziyang Song, Ziyi Gao, and Zizheng Pan. Deepseek-v3 technical report. *ArXiv*, abs/2412.19437, 2024. 3
- [12] Haiwen Diao, Yufeng Cui, Xiaotong Li, Yueze Wang, Huchuan Lu, and Xinlong Wang. Unveiling encoder-free vision-language models. *arXiv preprint arXiv:2406.11832*, 2024. 1, 2, 3
- [13] Haodong Duan, Junming Yang, Yuxuan Qiao, Xinyu Fang, Lin Chen, Yuan Liu, Xiaoyi Dong, Yuhang Zang, Pan Zhang, Jiaqi Wang, et al. Vlmevalkit: An open-source toolkit for evaluating large multi-modality models. In *Proceedings of the 32nd ACM International Conference on Multimedia*, pages 11198–11201, 2024. 5
- [14] Abhimanyu Dubey, Abhinav Jauhri, Abhinav Pandey, Abhishek Kadian, Ahmad Al-Dahle, Aiesha Letman, Akhil Mathur, Alan Schelten, Amy Yang, Angela Fan, Anirudh Goyal, Anthony S. Hartshorn, Aobo Yang, Archi Mitra, Archie Sravankumar, Artem Korenev, Arthur Hinsvark, Arun Rao, Aston Zhang, Aurélien Rodriguez, Austen Gregerson, Ava Spataru, Bap tiste Roziere, Bethany Biron, Binh Tang, Bobbie Chern, Charlotte Caucheteux, Chaya Nayak, Chloe Bi, Chris Marra, Chris McConnell, Christian Keller, Christophe Touret, Chunyang Wu, Corinne Wong, Cristian Cantón Ferrer, Cyrus Nikolaidis, Damien Allonsius, Daniel Song, Danielle Pintz, Danny Livshits, David Esiobu, Dhruv Choudhary, Dhruv Mahajan, Diego Garcia-Olano, Diego Perino, Dieuwke Hupkes, Egor Lakomkin, Ehab A. AlBadawy, Elina Lobanova, Emily Dinan, Eric Michael Smith, Filip Radenovic, Frank Zhang, Gabriele Synnaeve, Gabrielle Lee, Georgia Lewis Anderson, Graeme Nail, Grégoire Mialon, Guanglong Pang, Guillem Cucurell, Hailey Nguyen, Hannah Korevaar, Hu Xu, Hugo Touvron, Iliyan Zarov, Imanol Arrieta Ibarra, Isabel M. Kloumann, Ishan Misra, Ivan Evtimov, Jade Copet, Jaewon Lee, Jan Laurens Geffert, Jana Vranes, Jason Park, Jay Mahadeokar, Jeet Shah, Jelmer van der Linde, Jennifer Billock, Jenny Hong, Jenya Lee, Jeremy Fu, Jianfeng Chi, Jianyu Huang, Jiawen Liu, Jie Wang, Jiecao Yu, Joanna Bitton, Joe Spisak, Jongsoo Park, Joseph Rocca, Joshua Johnstun, Joshua Saxe, Ju-Qing Jia, Kalyan Vasuden Alwala, K. Upasani, Kate Plawiak, Keqian Li, Ken-591 neth Heafield, Kevin Stone, Khalid El-Arini, Krithika Iyer, Kshitiz Malik, Kuen ley Chiu, Kunal Bhalla, Lauren Rantala-Yearly, Laurens van der Maaten, Lawrence Chen, Liang Tan, Liz Jenkins, Louis Martin, Lovish Madaan, Lubo Malo, Lukas Blecher, Lukas Landzaat, Luke de Oliveira, Madeline Muzzi, Mahesh Babu Pasupuleti, Mannat Singh, Manohar Paluri, Marcin Kardas, Mathew Oldham, Mathieu Rita, Maya Pavlova, Melissa Hall Melanie Kambadur, Mike Lewis, Min Si, Mitesh Kumar Singh, Mona Hassan, Naman Goyal, Narjes Torabi, Nikolay Bashlykov, Nikolay Bogoychev, Niladri S. Chatterji, Olivier Duchenne, Onur cCelebi, Patrick Alrassy, Pengchuan Zhang, Pengwei Li, Petar Vasić, Peter Weng, Prajjwal Bhargava, Pratik Dubal, Praveen Krishnan, Punit Singh Koura, Puxin Xu, Qing He, Qingxiao Dong, Ragavan Srinivasan, Raj Ganapathy, Ramon Calderer, Ricardo Silveira Cabral, Robert Stojnic, Roberta Raileanu, Rohit Girdhar, Rohit Patel, Ro main Sauvestre, Ronnie Polidoro, Roshan Sumbaly, Ross Taylor, Ruan Silva, Rui Hou, Rui Wang, Saghar Hosseini, Sahana Chennabas-

appa, Sanjay Singh, Sean Bell, Seohyun Sonia Kim, Sergey Edunov, Shaoliang Nie, Sharan Narang, Sharath Chandra Raparthy, Sheng Shen, Shengye Wan, Shruti Bhosale, Shun Zhang, Simon Vandenhende, Soumya Batra, Spencer Whitman, Sten Sootla, Stephane Collot, Suchin Gururangan, Sydney Borodinsky, Tamar Herman, Tara Fowler, Tarek Sheasha, Thomas Georgiou, Thomas Scialom, Tobias Speckbacher, Todor Mihaylov, Tong Xiao, Ujjwal Karn, Vedanuj Goswami, Vibhor Gupta, Vignesh Ramanathan, Viktor Kerkez, Vincent Gouget, Virginie Do, Vish Vogeti, Vladan Petrovic, Weiwei Chu, Wenhan Xiong, Wenyin Fu, Whitney Meers, Xavier Martinet, Xiaodong Wang, Xiaoqing Ellen Tan, Xinfeng Xie, Xuchao Jia, Xuwei Wang, Yaelle Goldschlag, Yashesh Gaur, Yasmine Babaei, Yiqian Wen, Yiwen Song, Yuchen Zhang, Yue Li, Yuning Mao, Zacharie Delpierre Coudert, Zhengxu Yan, Zhengxing Chen, Zoe Papakipos, Aaditya K. Singh, Aaron Grattafori, Abha Jain, Adam Kelsey, Adam Shajnfeld, Adi Gangidi, Adolfo Victoria, Ahuva Goldstand, Ajay Menon, Ajay Sharma, Alex Boesenberg, Alex Vaughan, Alexei Baevski, Allie Feinstein, Amanda Kallet, Amit Sangani, Anam Yunus, Andrei Lupu, Andres Alvarado, Andrew Caples, Andrew Gu, Andrew Ho, Andrew Poulton, Andrew Ryan, Ankit Ramchandani, Annie Franco, Aparajita Saraf, Arkabandhu Chowdhury, Ashley Gabriel, Ashwin Bharambe, Assaf Eisenman, Azadeh Yazdan, Beau James, Ben Maurer, Ben Leonhardi, Po-Yao (Bernie) Huang, Beth Loyd, Beto De Paola, Bhargavi Paranjape, Bing Liu, Bo Wu, Boyu Ni, Braden Hancock, Bram Wasti, Brandon Spence, Brani Stojkovic, Brian Gamido, Britt Montalvo, Carl Parker, Carly Burton, Catalina Mejia, Changhan Wang, Changkyu Kim, Chao Zhou, Chester Hu, Ching-Hsiang Chu, Chris Cai, Chris Tindal, Christoph Feichtenhofer, Damon Civin, Dana Beaty, Daniel Kreymer, Shang-Wen Li, Danny Wyatt, David Adkins, David Xu, Davide Testuggine, Delia David, Devi Parikh, Diana Liskovich, Didem Foss, Dingkan Wang, Duc Le, Dustin Holland, Edward Dowling, Eissa Jamil, Elaine Montgomery, Eleonora Presani, Emily Hahn, Emily Wood, Erik Brinkman, Esteban Arcaute, Evan Dunbar, Evan Smothers, Fei Sun, Felix Kreuk, Feng Tian, Firat Ozgenel, Francesco Caggioni, Francisco Guzman, Frank J. Kanayet, Frank Seide, Gabriela Medina Florez, Gabriella Schwarz, Gada Badeer, Georgia Swee, Gil Halpern, Govind Thattai, Grant Herman, Grigory G. Sizov, Guangyi Zhang, Guna Lakshminarayanan, Hamid Shojanazeri, Han Zou, Hannah Wang, Han Zha, Haroun Habeeb, Harrison Rudolph, Helen Suk, Henry Aspegren, Hunter Goldman, Igor Molybog, Igor Tufanov, Irina-Elena Veliche, Itai Gat, Jake Weissman, James Geboski, James Kohli, Japhet Asher, Jean-Baptiste Gaya, Jeff Marcus, Jeff Tang, Jennifer Chan, Jenny Zhen, Jeremy Reizenstein, Jeremy Teboul, Jessica Zhong, Jian Jin, Jingyi Yang, Joe Cummings, Jon Carvill, Jon Shepard, Jonathan McPhie, Jonathan Torres, Josh Ginsburg, Junjie Wang, Kaixing(Kai) Wu, U KamHou, Karan Saxena, Karthik Prasad, Kartikay Khandelwal, Katayoun Zand, Kathy Matosich, Kaushik Veeraraghavan, Kelly Michelena, Keqian Li, Kun Huang, Kunal Chawla, Kushal Lakhotia, Kyle Huang, Lailin Chen, Lakshya Garg, A Lavender, Leandro Silva, Lee Bell, Lei Zhang, Liangpeng Guo, Licheng Yu, Liron Moshkovich, Luca Wehrstedt, Madian Khabsa,

Manav Avalani, Manish Bhatt, Maria Tsimpoukelli, Martynas Mankus, Matan Hasson, Matthew Lennie, Matthias Reso, Maxim Groshev, Maxim Naumov, Maya Lathi, Meghan Keneally, Michael L. Seltzer, Michal Valko, Michelle Restrepo, Mihir Patel, Mik Vyatskov, Mikayel Samvelyan, Mike Clark, Mike Macey, Mike Wang, Miquel Jubert Hermoso, Mo Metanat, Mohammad Rastegari, Munish Bansal, Nandhini Santhanam, Natascha Parks, Natasha White, Navyata Bawa, Nayan Singhal, Nick Egebo, Nicolas Usunier, Nikolay Pavlovich Laptev, Ning Dong, Ning Zhang, Norman Cheng, Oleg Chernoguz, Olivia Hart, Omkar Salpekar, Ozlem Kalinli, Parkin Kent, Parth Parekh, Paul Saab, Pavan Balaji, Pedro Rittner, Philip Bontrager, Pierre Roux, Piotr Dollár, Polina Zvyagina, Prashant Ratanchandani, Pritish Yuvraj, Qian Liang, Rachad Alao, Rachel Rodriguez, Rafi Ayub, Raghotham Murthy, Raghu Nayani, Rahul Mitra, Raymond Li, Rebekkah Hogan, Robin Battey, Rocky Wang, Rohan Maheswari, Russ Howes, Ruty Rinott, Sai Jayesh Bondu, Samyak Datta, Sara Chugh, Sara Hunt, Sargun Dhillon, Sasha Sidorov, Satadru Pan, Saurabh Verma, Seiji Yamamoto, Sharadh Ramaswamy, Shaun Lindsay, Sheng Feng, Shenghao Lin, Shengxin Cindy Zha, Shiva Shankar, Shuqiang Zhang, Sinong Wang, Sneha Agarwal, Soji Sajuyigbe, Soumith Chintala, Stephanie Max, Stephen Chen, Steve Kehoe, Steve Satterfield, Sudarshan Govindaprasad, Sumit Gupta, Sung-Bae Cho, Sunny Virk, Suraj Subramanian, Sy Choudhury, Sydney Goldman, Tal Remez, Tamar Glaser, Tamara Best, Thilo Kohler, Thomas Robinson, Tianhe Li, Tianjun Zhang, Tim Matthews, Timothy Chou, Tzook Shaked, Varun Vontimitta, Victoria Ajayi, Victoria Montanez, Vijai Mohan, Vinay Satish Kumar, Vishal Mangla, Vlad Ionescu, Vlad Andrei Poenaru, Vlad T. Mihailescu, Vladimir Ivanov, Wei Li, Wenchen Wang, Wenwen Jiang, Wes Bouaziz, Will Constable, Xia Tang, Xiaofang Wang, Xiaoqian Wu, Xiaolan Wang, Xide Xia, Xilun Wu, Xinbo Gao, Yanjun Chen, Ye Hu, Ye Jia, Ye Qi, Yenda Li, Yilin Zhang, Ying Zhang, Yossi Adi, Youngjin Nam, Yu Wang, Yuchen Hao, Yundi Qian, Yuzi He, Zach Rait, Zachary DeVito, Zef Rosnbrick, Zhaoduo Wen, Zhenyu Yang, and Zhiwei Zhao. The llama 3 herd of models. *ArXiv*, abs/2407.21783, 2024. 3

- [15] Patrick Esser, Robin Rombach, and Bjorn Ommer. Taming transformers for high-resolution image synthesis. In *CVPR*, pages 12873–12883, 2021. 3
- [16] Chaoyou Fu, Peixian Chen, Yunhang Shen, Yulei Qin, Mengdan Zhang, Xu Lin, Zhenyu Qiu, Wei Lin, Jinrui Yang, Xiawu Zheng, Ke Li, Xing Sun, and Rongrong Ji. MME: A comprehensive evaluation benchmark for multimodal large language models. *arXiv: 2306.13394*, 2023. 2, 3, 5, 14
- [17] Tianrui Guan, Fuxiao Liu, Xiyang Wu, Ruiqi Xian, Zongxia Li, Xiaoyu Liu, Xijun Wang, Lichang Chen, Furong Huang, Yaser Yacoub, Dinesh Manocha, and Tianyi Zhou. Hallusionbench: An advanced diagnostic suite for entangled language hallucination and visual illusion in large vision-language models. *2024 IEEE/CVF Conference on Computer Vision and Pattern Recognition (CVPR)*, pages 14375–14385, 2023. 5
- [18] Muyang He, Yexin Liu, Boya Wu, Jianhao Yuan, Yueze Wang, Tiejun Huang, and Bo Zhao. Efficient multimodal learning

- from data-centric perspective. *ArXiv*, abs/2402.11530, 2024. 3
- [19] Drew A. Hudson and Christopher D. Manning. GQA: A new dataset for real-world visual reasoning and compositional question answering. In *CVPR*, pages 6700–6709, 2019. 3
- [20] Aniruddha Kembhavi, Mike Salvato, Eric Kolve, Minjoon Seo, Hannaneh Hajishirzi, and Ali Farhadi. A diagram is worth a dozen images. In *ECCV*, pages 235–251, 2016. 3, 5
- [21] Hugo Laurençon, Léo Tronchon, Matthieu Cord, and Victor Sanh. What matters when building vision-language models?, 2024. 5
- [22] Bo Li, Kaichen Zhang, Hao Zhang, Dong Guo, Renrui Zhang, Feng Li, Yuanhan Zhang, Ziwei Liu, and Chunyuan Li. Llava-next: Stronger llms supercharge multimodal capabilities in the wild, 2024. 2
- [23] Bo Li, Yuanhan Zhang, Dong Guo, Renrui Zhang, Feng Li, Hao Zhang, Kaichen Zhang, Yanwei Li, Ziwei Liu, and Chunyuan Li. Llava-onevision: Easy visual task transfer. *ArXiv*, abs/2408.03326, 2024. 5
- [24] Haotian Liu, Chunyuan Li, Yuheng Li, and Yong Jae Lee. Improved baselines with visual instruction tuning. *arXiv: 2310.03744*, 2023. 1, 2, 3
- [25] Haotian Liu, Chunyuan Li, Qingyang Wu, and Yong Jae Lee. Visual instruction tuning. In *NeurIPS*, 2023. 2
- [26] Haotian Liu, Chunyuan Li, Yuheng Li, Bo Li, Yuanhan Zhang, Sheng Shen, and Yong Jae Lee. Llava-next: Improved reasoning, ocr, and world knowledge, 2024. 1, 3
- [27] Yuan Liu, Haodong Duan, Yuanhan Zhang, Bo Li, Songyang Zhang, Wangbo Zhao, Yike Yuan, Jiaqi Wang, Conghui He, Ziwei Liu, Kai Chen, and Dahua Lin. Mmbench: Is your multi-modal model an all-around player? *arXiv: 2307.06281*, 2023. 3, 5
- [28] Yuliang Liu, Zhang Li, Biao Yang, Chunyuan Li, Xucheng Yin, Cheng-lin Liu, Lianwen Jin, and Xiang Bai. On the hidden mystery of ocr in large multimodal models. *arXiv preprint arXiv:2305.07895*, 2023. 2
- [29] Haoyu Lu, Wen Liu, Bo Zhang, Bingxuan Wang, Kai Dong, Bo Liu, Jingxiang Sun, Tongzheng Ren, Zhuoshu Li, Hao Yang, Yaofeng Sun, Chengqi Deng, Hanwei Xu, Zhenda Xie, and Chong Ruan. Deepseek-vl: Towards real-world vision-language understanding. *arXiv: 2403.05525*, 2024. 1, 3
- [30] Pan Lu, Swaroop Mishra, Tony Xia, Liang Qiu, Kai-Wei Chang, Song-Chun Zhu, Oyvind Tafjord, Peter Clark, and Ashwin Kalyan. Learn to explain: Multimodal reasoning via thought chains for science question answering. In *NeurIPS*, 2022. 5
- [31] Gen Luo, Xue Yang, Wenhan Dou, Zhaokai Wang, Jifeng Dai, Yu Qiao, and Xizhou Zhu. Mono-intervl: Pushing the boundaries of monolithic multimodal large language models with endogenous visual pre-training. *arXiv preprint arXiv:2410.08202*, 2024. 1, 2, 3
- [32] Anand Mishra, Shashank Shekhar, Ajeet Kumar Singh, and Anirban Chakraborty. Ocr-vqa: Visual question answering by reading text in images. In *ICDAR*, pages 947–952, 2019. 2
- [33] Alec Radford, Jong Wook Kim, Chris Hallacy, Aditya Ramesh, Gabriel Goh, Sandhini Agarwal, Girish Sastry, Amanda Askell, Pamela Mishkin, Jack Clark, Gretchen Krueger, and Ilya Sutskever. Learning transferable visual models from natural language supervision. In *ICML*, pages 8748–8763, 2021. 1, 2, 3, 15
- [34] Zhihong Shao, Damai Dai, Daya Guo, Bo Liu (Benjamin Liu), Zihan Wang, and Huajian Xin. Deepseek-v2: A strong, economical, and efficient mixture-of-experts language model. *ArXiv*, abs/2405.04434, 2024. 3
- [35] Noam M. Shazeer, Azalia Mirhoseini, Krzysztof Maziarz, Andy Davis, Quoc V. Le, Geoffrey E. Hinton, and Jeff Dean. Outrageously large neural networks: The sparsely-gated mixture-of-experts layer. *ArXiv*, abs/1701.06538, 2017. 3
- [36] Amanpreet Singh, Vivek Natarajan, Meet Shah, Yu Jiang, Xinlei Chen, Dhruv Batra, Devi Parikh, and Marcus Rohrbach. Towards VQA models that can read. In *CVPR*, 2019. 5
- [37] Chameleon Team. Chameleon: Mixed-modal early-fusion foundation models. *arXiv preprint arXiv:2405.09818*, 2024. 3
- [38] Gemini Team, Rohan Anil, Sebastian Borgeaud, Yonghui Wu, Jean-Baptiste Alayrac, Jiahui Yu, Radu Soricut, Johan Schalkwyk, Andrew M Dai, Anja Hauth, et al. Gemini: a family of highly capable multimodal models. *arXiv: 2312.11805*, 2023. 1, 3
- [39] Shengbang Tong, Ellis L Brown, Penghao Wu, Sanghyun Woo, Manoj Middepogu, Sai Charitha Akula, Jihan Yang, Shusheng Yang, Adithya Iyer, Xichen Pan, Austin Wang, Rob Fergus, Yann LeCun, and Saining Xie. Cambrian-1: A fully open, vision-centric exploration of multimodal llms. *ArXiv*, abs/2406.16860, 2024. 5
- [40] Michael Tschanen, Alexey Gritsenko, Xiao Wang, Muhammad Ferjad Naeem, Ibrahim Alabdulmohsin, Nikhil Parthasarathy, Talfan Evans, Lucas Beyer, Ye Xia, Basil Mustafa, Olivier Hénaff, Jeremiah Harmsen, Andreas Steiner, and Xiaohua Zhai. Siglip 2: Multilingual vision-language encoders with improved semantic understanding, localization, and dense features. *arXiv preprint arXiv:2502.14786*, 2025. 15
- [41] Aaron Van Den Oord, Oriol Vinyals, et al. Neural discrete representation learning. *NeurIPS*, 30, 2017. 3
- [42] Peng Wang, Shuai Bai, Sinan Tan, Shijie Wang, Zhihao Fan, Jinze Bai, Keqin Chen, Xuejing Liu, Jialin Wang, Wenbin Ge, et al. Qwen2-vl: Enhancing vision-language model’s perception of the world at any resolution. *arXiv preprint arXiv:2409.12191*, 2024. 1, 3
- [43] Xinlong Wang, Xiaosong Zhang, Zhengxiong Luo, Quan Sun, Yufeng Cui, Jinsheng Wang, Fan Zhang, Yueze Wang, Zhen Li, Qiyang Yu, et al. Emu3: Next-token prediction is all you need. *arXiv preprint arXiv:2409.18869*, 2024. 3
- [44] Jinheng Xie, Weijia Mao, Zechen Bai, David Junhao Zhang, Weihao Wang, Kevin Qinghong Lin, Yuchao Gu, Zhijie Chen, Zhenheng Yang, and Mike Zheng Shou. Show-o: One single transformer to unify multimodal understanding and generation. *arXiv preprint arXiv:2408.12528*, 2024. 3
- [45] Qwen An Yang, Baosong Yang, Beichen Zhang, Binyuan Hui, Bo Zheng, Bowen Yu, Chengyuan Li, Dayiheng Liu, Fei Huang, Guanting Dong, Haoran Wei, Huan Lin, Jian Yang, Jianhong Tu, Jianwei Zhang, Jianxin Yang, Jiaxin Yang,

- Jingren Zhou, Junyang Lin, Kai Dang, Keming Lu, Keqin Bao, Kexin Yang, Le Yu, Mei Li, Mingfeng Xue, Pei Zhang, Qin Zhu, Rui Men, Runji Lin, Tianhao Li, Tingyu Xia, Xingzhang Ren, Xuancheng Ren, Yang Fan, Yang Su, Yi-Chao Zhang, Yunyang Wan, Yuqi Liu, Zeyu Cui, Zhenru Zhang, Zihan Qiu, Shanghaoran Quan, and Zekun Wang. Qwen2.5 technical report. *ArXiv*, abs/2412.15115, 2024. [3](#)
- [46] Weihao Yu, Zhengyuan Yang, Linjie Li, Jianfeng Wang, Kevin Lin, Zicheng Liu, Xinchao Wang, and Lijuan Wang. Mm-vet: Evaluating large multimodal models for integrated capabilities. *arXiv: 2308.02490*, 2023. [3](#), [5](#), [7](#)
- [47] Xiang Yue, Yuansheng Ni, Kai Zhang, Tianyu Zheng, Ruoqi Liu, Ge Zhang, Samuel Stevens, Dongfu Jiang, Weiming Ren, Yuxuan Sun, et al. Mmmu: A massive multi-discipline multi-modal understanding and reasoning benchmark for expert agi. *arXiv: 2311.16502*, 2023. [3](#), [5](#)
- [48] Xiaohua Zhai, Basil Mustafa, Alexander Kolesnikov, and Lucas Beyer. Sigmoid loss for language image pre-training. In *ICCV*, pages 11975–11986, 2023. [2](#), [15](#)

## A. Appendix Section

### A.1. Ablation on Combination Design

To optimize the performance when inclusion of multi-grained learnable queries, we ablate on different design choice for the combination as shown in Table 4. From the experiment results, we observe that both the order of the granularity and the combination method matters. From the first row and the second row, there is a performance drop when the finer-grained learnable queries are placed nearer the instruction text and farer from the images, which is intuitive as images are much more fine-grain than high-level text in terms of semantics. Therefore, placing finer-grained query nearer the images can have a better transition from low-level to high-level understanding.

We also try not concatenating the learnable queries of different granularity together, but align them from the same fine-grained sequence before and after average pooling according to the unflattened sequence, which is shown in the third row of Table 4. The performance also draws a little compared to concatenate different learnable queries together.

And finally, we choose concatenate learnable queries with stride size 3 and 4 together, which achieves highest score according to the experiments.

### A.2. Effect of Learnable Queries with Different Granularity

We demonstrate more results on the inclusion of learnable queries with different granularity on different sub-tasks of MME [16] in Table 5 and Table 6. According to the results, we can find that finer-grained learnable queries (with patch size 2) can benefit more on the tasks requiring fine-grained recognition like OCR, numerical calculation and code reasoning. While coarse learnable queries will have an advantage on high-level understanding tasks, like color, posters, or artwork recognition and commonsense reasoning.

### A.3. Visualization

#### A.3.1. Visualization Overall Results with Radar Chart

We visualize the performance of encoder-free MLLMs and the selected top 2 encoder-based MLLMs in Figure 6. It is obvious to see that BREEN performs comparable with a strong encoder-based baseline, which is Cambrian.

#### A.3.2. Visualization of Attention Weights

We visualize the attention weights from the critical output tokens to all the image tokens and the learnable query tokens in Figure 7. The first row of each example is the visualization for image tokens and the second row is for learnable queries. We can observe from the visualization that it is hard for attention weights to focus on the desired area in the first layer, they just distribute randomly with a higher average score. And we find that the attention to image tokens will

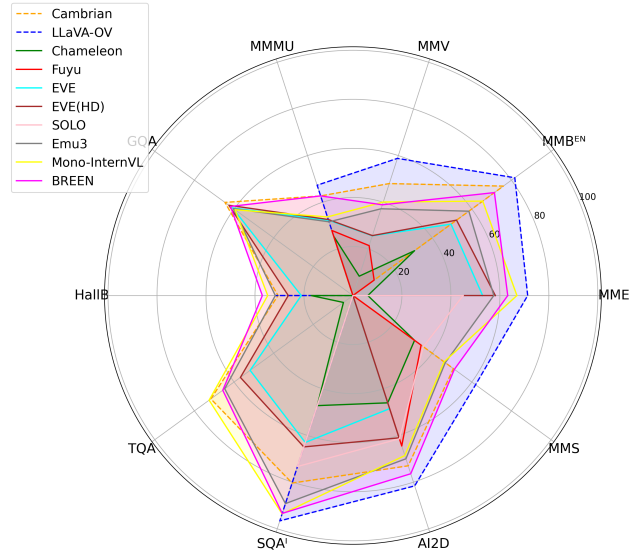


Figure 6. Comparison of the performance of BREEN with encoder-based and encoder-free models.

refine to a specific area in the last layer, while still attending to a wider area in the middle layer. On the other hand, the attention scores to the learnable query can actively and correctly identify the important areas in the middle layer, but fade out in the last year. It is likely to be explained by the different granularity of the learnable query and image tokens.

### A.4. Limitation and Future Plan

While BREEN presents a significant step toward data-efficient encoder-free multimodal learning, several limitations remain, providing avenues for future research.

#### Adaptive Query Selection for Task-Specific Needs

BREEN employs a dual-granularity learnable query mechanism, allowing the model to leverage both fine-grained and coarse-grained representations for different multimodal tasks. However, the current approach lacks an explicit mechanism for dynamically selecting or weighting queries based on the task context. Future work could explore adaptive query selection strategies, such as attention-based weighting or reinforcement learning-based query routing, to optimize query utilization based on task requirements.

#### Efficient Token Utilization and Sequence Compression

One limitation of BREEN is that the addition of learnable queries increases the token sequence length, leading to higher computational costs during training and inference. Although learnable queries improve vision-language alignment, their fixed length may introduce redundancy, especially for tasks with varying levels of visual detail. To address this,

Stride Size	Align Method	SQA <sup>1</sup>	TQA	GQA	MME
4 & 2	Concat	62.8	41.0	50.8	1278.1
2 & 4	Concat	63.2	41.2	51.2	1290.4
2 & 4	AvgPool	63.1	40.9	51.0	1262.7
3 & 4	Concat	63.7	41.4	51.7	1333.4

Table 4. Ablation study of BREEN on the combination design for learnable queries with different granularity.

Stride/Patch Size	existence	count	position	color	posters	celebrity	scene	landmark	artwork	ocr	Total
2 (12 × 12)	173.3	88.3	78.3	101.6	56.5	47.1	139.0	82.5	85.8	67.5	919.9
3 (8 × 8)	175.0	88.3	101.7	111.7	62.9	62.6	138.3	104.3	86.8	57.5	989.0
4 (6 × 6)	175.0	90.0	98.3	145.0	68.4	47.4	134.3	85.3	90.8	57.5	991.8

Table 5. Sub-task performance on MME-P.

future work could explore mechanisms for adaptive query compression, where the model dynamically selects or merges learnable queries based on task requirements. Additionally, compressing image tokens alongside learnable queries could further enhance efficiency while retaining critical visual information.

**Exploring Stronger Vision Encoder Teachers** BREEN distills visual knowledge from CLIP [33] to enhance alignment in an encoder-free setting. However, recent advancements in vision encoders, such as SigLIP and SigLIP2 [40, 48], have demonstrated superior visual representations with stronger semantic understanding. Future work could explore using these more powerful vision encoders as teachers to further improve the quality of learnable queries, potentially leading to better multimodal reasoning and more robust performance across diverse tasks.

Stride/Patch Size	common sense reasoning	numerical calculation	text translation	code reasoning	Total
2 (12 × 12)	70.0	50.0	95.0	87.5	302.5
3 (8 × 8)	72.1	42.5	110.0	80.0	304.64
4 (6 × 6)	83.6	47.5	72.5	55.0	258.57

Table 6. Sub-task performance on MME-C.

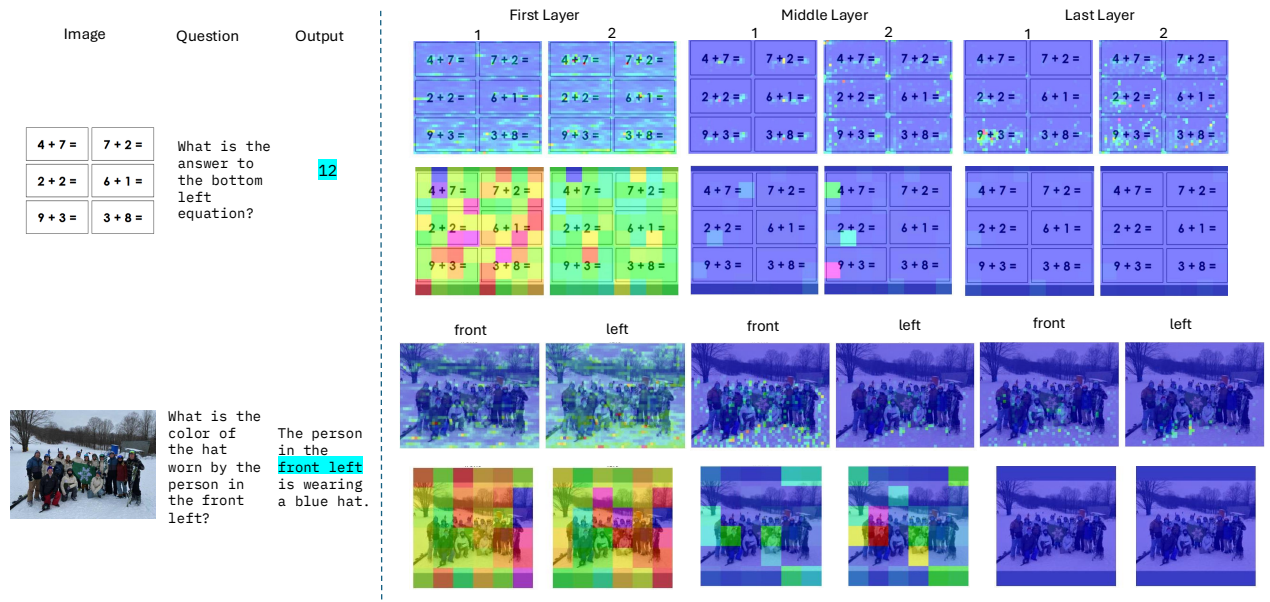


Figure 7. The output attention visualization to image tokens and learnable query tokens in different layers.



# BREEN: Bridge Data-Efficient Encoder-Free Multimodal Learning with Learnable Queries

## Supplementary Material

### A. Appendix Section

#### A.1. Ablation on Combination Design

To optimize the performance when inclusion of multi-grained learnable queries, we ablate on different design choice for the combination as shown in Table 1. From the experiment results, we observe that both the order of the granularity and the combination method matters. From the first row and the second row, there is a performance drop when the finer-grained learnable queries are placed nearer the instruction text and farer from the images, which is intuitive as images are much more fine-grain than high-level text in terms of semantics. Therefore, placing finer-grained query nearer the images can have a better transition from low-level to high-level understanding.

We also try not concatenating the learnable queries of different granularity together, but align them from the same fine-grained sequence before and after average pooling according to the unflattened sequence, which is shown in the third row of Table 1. The performance also draws a little compared to concatenate different learnable queries together.

And finally, we choose concatenate learnable queries with stride size 3 and 4 together, which achieves highest score according to the experiments.

#### A.2. Effect of Learnable Queries with Different Granularity

We demonstrate more results on the inclusion of learnable queries with different granularity on different sub-tasks of MME [?] in Table 2 and Table 3. According to the results, we can find that finer-grained learnable queries (with patch size 2) can benefit more on the tasks requiring fine-grained recognition like OCR, numerical calculation and code reasoning. While coarse learnable queries will have an advantage on high-level understanding tasks, like color, posters, or artwork recognition and commonsense reasoning.

### A.3. Visualization

#### A.3.1. Visualization Overall Results with Radar Chart

We visualize the performance of encoder-free MLLMs and the selected top 2 encoder-based MLLMs in Figure 1. It is obvious to see that BREEN performs comparable with a strong encoder-based baseline, which is Cambrian.

#### A.3.2. Visualization of Attention Weights

We visualize the attention weights from the critical output tokens to all the image tokens and the learnable query tokens

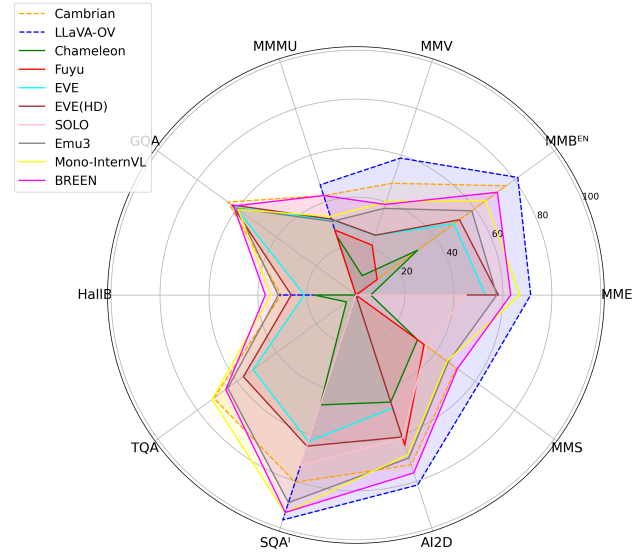


Figure 1. Comparison of the performance of BREEN with encoder-based and encoder-free models.

in Figure 2. The first row of each example is the visualization for image tokens and the second row is for learnable queries. We can observe from the visualization that it is hard for attention weights to focus on the desired area in the first layer, they just distribute randomly with a higher average score. And we find that the attention to image tokens will refine to a specific area in the last layer, while still attending to a wider area in the middle layer. On the other hand, the attention scores to the learnable query can actively and correctly identify the important areas in the middle layer, but fade out in the last year. It is likely to be explained by the different granularity of the learnable query and image tokens.

#### A.4. Limitation and Future Plan

While BREEN presents a significant step toward data-efficient encoder-free multimodal learning, several limitations remain, providing avenues for future research.

#### Adaptive Query Selection for Task-Specific Needs

BREEN employs a dual-granularity learnable query mechanism, allowing the model to leverage both fine-grained and coarse-grained representations for different multimodal tasks. However, the current approach lacks an explicit mechanism for dynamically selecting or weighting queries based on

Stride Size	Align Method	SQA <sup>1</sup>	TQA	GQA	MME
4 & 2	Concat	62.8	41.0	50.8	1278.1
2 & 4	Concat	63.2	41.2	51.2	1290.4
2 & 4	AvgPool	63.1	40.9	51.0	1262.7
3 & 4	Concat	63.7	41.4	51.7	1333.4

Table 1. Ablation study of BREEN on the combination design for learnable queries with different granularity.

Stride/Patch Size	existence	count	position	color	posters	celebrity	scene	landmark	artwork	ocr	Total
2 (12 × 12)	173.3	88.3	78.3	101.6	56.5	47.1	139.0	82.5	85.8	67.5	919.9
3 (8 × 8)	175.0	88.3	101.7	111.7	62.9	62.6	138.3	104.3	86.8	57.5	989.0
4 (6 × 6)	175.0	90.0	98.3	145.0	68.4	47.4	134.3	85.3	90.8	57.5	991.8

Table 2. Sub-task performance on MME-P.

067 the task context. Future work could explore adaptive query  
 068 selection strategies, such as attention-based weighting or re-  
 069 inforcement learning-based query routing, to optimize query  
 070 utilization based on task requirements.

071 **Efficient Token Utilization and Sequence Compression**

072 One limitation of BREEN is that the addition of learn-  
 073 able queries increases the token sequence length, leading to  
 074 higher computational costs during training and inference. Al-  
 075 though learnable queries improve vision-language alignment,  
 076 their fixed length may introduce redundancy, especially for  
 077 tasks with varying levels of visual detail. To address this,  
 078 future work could explore mechanisms for adaptive query  
 079 compression, where the model dynamically selects or merges  
 080 learnable queries based on task requirements. Additionally,  
 081 compressing image tokens alongside learnable queries could  
 082 further enhance efficiency while retaining critical visual in-  
 083 formation.

084 **Exploring Stronger Vision Encoder Teachers** BREEN

085 distills visual knowledge from CLIP [?] to enhance align-  
 086 ment in an encoder-free setting. However, recent advance-  
 087 ments in vision encoders, such as SigLIP and SigLIP2 [?  
 088 ? ], have demonstrated superior visual representations with  
 089 stronger semantic understanding. Future work could explore  
 090 using these more powerful vision encoders as teachers to  
 091 further improve the quality of learnable queries, potentially  
 092 leading to better multimodal reasoning and more robust per-  
 093 formance across diverse tasks.

Stride/Patch Size	common sense reasoning	numerical calculation	text translation	code reasoning	Total
2 (12 × 12)	70.0	50.0	95.0	87.5	302.5
3 (8 × 8)	72.1	42.5	110.0	80.0	304.64
4 (6 × 6)	83.6	47.5	72.5	55.0	258.57

Table 3. Sub-task performance on MME-C.

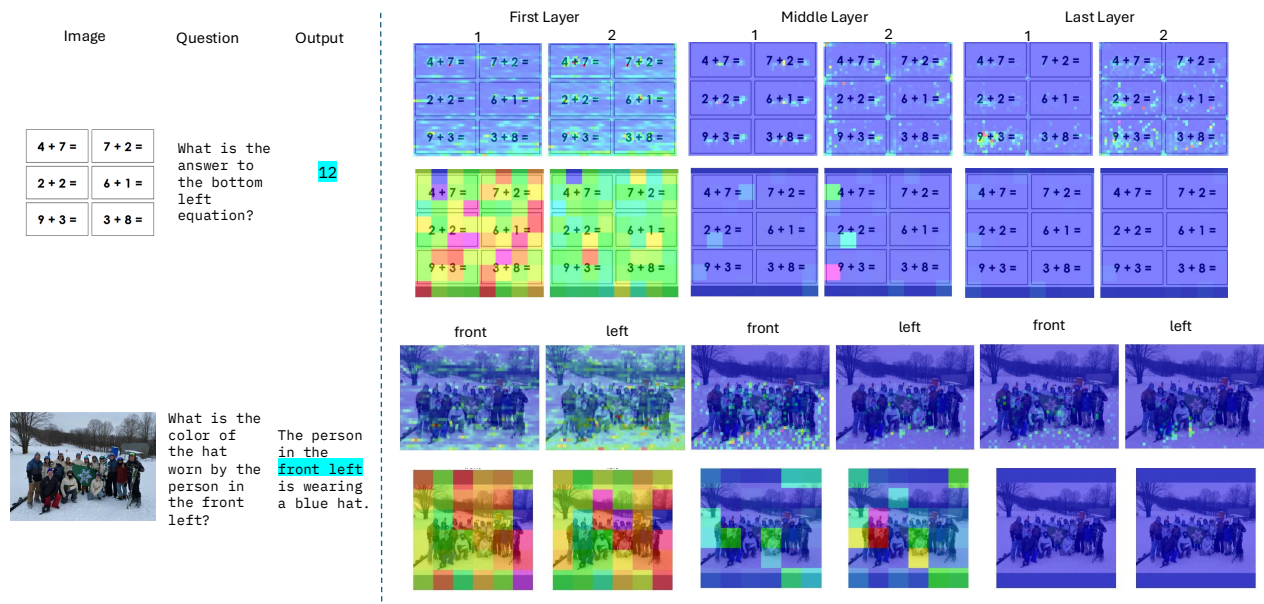


Figure 2. The output attention visualization to image tokens and learnable query tokens in different layers.